SolarPACES 2022, 28th International Conference on Concentrating Solar Power and Chemical Energy Systems
Thermal Energy Storage Materials, Media, and Systems
https://doi.org/10.52825/solarpaces.v1i.743

Published: 09 Feb. 2024

# Design of a Continuous Electrochemical Purification Reactor for Corrosion Mitigation in Molten Chloride Salt Systems

Liam Witteman[1,2][https://orcid.org/0000-0001-8450-8263], Kerry Rippy[2][https://orcid.org/0000-0001-7154-6543], Evan Ogren[3][https://orcid.org/0000-0002-9529-3154], Mark Anderson[3][https://orcid.org/0000-0002-8483-2714], Patrick Taylor[1], and Judith Vidal[2][https://orcid.org/0000-00021-0591-3250]

[1] Colorado School of Mines, USA

[2] National Renewable Energy Laboratory, USA

[3] University of Wisconsin-Madison, USA

**Abstract.** The utility of molten chloride salts in concentrating solar power (CSP) is dependent on the ability to maintain low corrosive impurities. Without proper purification, the corrosion rates of containment alloys exceed the industry standard of corrosion—under 20 μm/year. An extensive body of literature focuses on the initial purification stage of molten chloride salts. However, occurrences such as maintenance, leaks, and so forth expose the salt to the atmosphere and reintroduce impurities. Therefore, it is critical to develop a purification strategy that can control impurity levels during CSP plant operation. Here we present the design and fabrication of a purification vessel to continuously remove impurities out of flowing molten salt.

**Keywords:** Molten Chloride Salts, Salt Purification, Electrowinning

## 1. Introduction

When molten chloride salt is exposed to air and moisture, corrosive impurities such as MgOHCl form within it [1, 2]. Thus, methods for controlling corrosion are essential for the progress of molten chloride salt systems. An acceptable threshold of corrosion (≤ 20 μm/year) can be obtained when MgOHCl concentrations are 1000 ppm or less [3, 4]. Chemical purification with molten Mg metal has been proven to be an effective treatment for removal of corrosive impurities, however, it is not viable below the melting point of Mg because of the slow kinetics [3, 4]. Therefore, an alternative corrosion control method has been proposed and demonstrated at laboratory scale, based on electrochemistry [5]. This method demonstrated significant opportunities for scaling up and for providing effective online corrosion control during operation of a concentrating solar power (CSP) plant.

In this method, bulk electropositive metal electrodes and electrical energy increase the dissolution kinetics of Mg into the molten chloride, overcoming the problems associated with operating temperatures below the active metallic Mg melting point. Under these conditions, the following reactions have been proposed as occurring:

$$2MgOHCl \rightarrow 2MgOH^{+} + 2Cl^{-} \quad \textit{[molten salt]} \quad (1)$$

$$Mg(s) \rightarrow Mg^{2+} + 2e^{-} \quad \textit{[anode]} \quad (2)$$

$$2MgOH^+ + 2e^- \rightarrow 2MgO + H_2(g) \quad \textit{[cathode]} \quad (3)$$

$$Mg^{2+} + 2Cl^- \rightarrow MgCl_2 \quad \textit{[molten salt]} \quad (4)$$

$$2MgOHCl + Mg(s) \rightarrow MgCl_2 + 2MgO + H_2(g) \quad \textit{[overall reaction]} \quad (5)$$

## 2. Batch Reactor Data

In a laboratory-scale batch reactor, the rate of MgOHCl removal via electrolysis was quantified electrochemically using cyclic voltammetry (CV) based on the methods of Ding et al. [6] and Guo et al. [7]. The experiments were conducted in salt batches of 550 g.

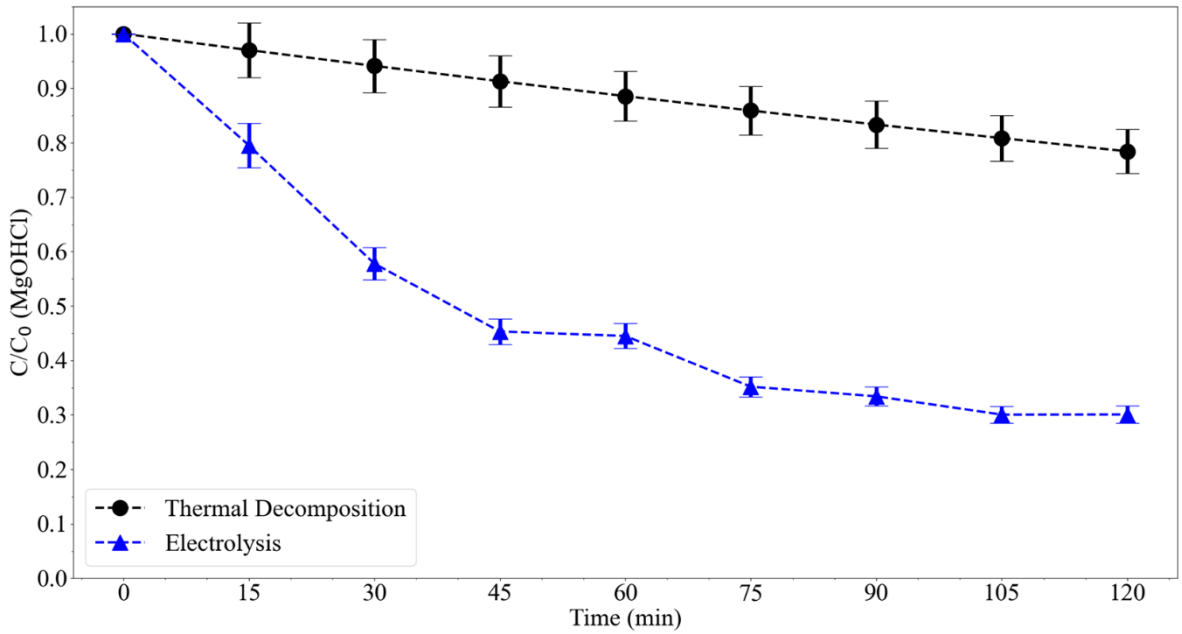


**Figure 1**. Comparing concentration of $MgOH^+$ impurity over time via electrolysis vs. natural decomposition at 500 ºC. Applied potential of Mg anode is -1.25 V vs. W.

From Figure 1, the electrolysis method was effective and reduced the concentration of $MgOH^+$ by 70% in a 2-hour experiment. The process was found to be effective under static conditions where the process was mass transfer controlled. The purification process is expected to further improve in a flow system due to enhanced mass transfer under flowing conditions. Furthermore, we did not observe noticeable passivation of the Tungsten (W) cathode based on the current density, indicative of a diffusion-controlled system. Based on optimized parameters, we found a limiting current density of 87 mA/cm$^2$.

The results in a laboratory-scale batch reactor (publication in progress) indicate that this electrochemical process could be effectively integrated into a flow system and scaled up to industrial molten-chloride salt systems. Thus, the primary objective of the work reported here is the design of a laboratory-scale electrochemical purification cell that operates under flowing conditions. Furthermore, we lay out the fundamental equations used to predict the performance of the reactor based on batch reactor data.

## 3. Reactor Design

For a diffusion-controlled electrode process, the limiting current density is based on the rate of mass transfer of the impurity $MgOH^+$ to the electrode surface. Under flowing conditions,

the rate of mass transfer is enhanced, and the amount of enhancement can be estimated using the Sherwood number ($Sh$).

$$Sh = \frac{k_m}{D_{MgOH^+}/L} \tag{6}$$

Where $k_m$ is the mass transfer coefficient (m/s), $\mathcal{D}_{MgOH^+}$ is the diffusion coefficient of $MgOH^+$ ($m^2/s$), and $L$ is the characteristic length (m). From cyclic voltammetry experiments, we calculated $\mathcal{D}_{MgOH^+}$ to be 1.103e-5 $cm^2/s$ at 500 ºC.

The mass transfer coefficient can be estimated using the Chilton-Colburn j-factor analogy for mass transfer, which has been shown to fit data well for diffusion-limited electrode processes with high Schmidt values (693–37,200) [8].

$$j_M = \frac{Sh}{ReSc^{1/3}\sqrt{\frac{f}{2}}} = 0.0575+0.1184Sc^{-\frac{1}{3}} \tag{7}$$

Where $j_M$ is the j-factor analogy for mass transfer, $Re$ is the Reynolds number, $Sc$ is the Schmidt number, and $f$ is the Fanning-friction factor.

The Reynolds number is calculated based on the fluid properties and the equivalent diameter of the reactor.

$$Re = \frac{\rho u D_e}{\mu} \tag{8}$$

Where $\rho$ is the density ($kg/m^3$), $u$ is the velocity (m/s), $D_e$ is the equivalent diameter (m), and $\mu$ is the viscosity (Pa·s).

The Schmidt number is calculated based on the fluid and $MgOH^+$ properties.

$$Sc = \frac{\mu}{\rho D_{MgOH^+}} \tag{9}$$

In our system the Schmidt number is 1813 at 500 ºC. This is considered a high Sc system and warrants a different mass transfer correlation presented in Eq. 7.

The equivalent diameter, $D_e$, is defined as

$$D_e = 4r_H = \frac{D_{reactor}^2}{(D_{reactor}+n_{elec}D_{elec})} \tag{10}$$

Where $r_H$ is the hydraulic radius.

$$r_H = \frac{A}{S} = \frac{\frac{\pi}{4}D_{reactor}^2}{\pi(D_{reactor}+n_{elec}D_{elec})} = \frac{D_{reactor}^2}{4(D_{reactor}+n_{elec}D_{elec})} \tag{11}$$

Where $A$ is the cross-sectional area of the flow, S is the wetted perimeter of the cross section, $D_{reactor}$ is the diameter of the reactor vessel, $D_{elec}$ is the diameter of the electrode, and $n_{elec}$ is the number of electrodes.

In the flow experiments, the salt flow rate will vary from 0.1 to 1 gpm, resulting in Re numbers ranging from 34.6 to 346. At these flow rates the flow is presumed laminar within the reactor, and leads to the following expression for the friction factor.

$$f = \frac{16}{Re} \tag{12}$$

Furthermore, the mean residence time of the reactor is important to estimate the salt throughput.

$$\tau = \frac{V}{Q} \tag{13}$$

Where $\tau$ is the mean residence time (s), $V$ is the volume of the reactor ($m^3$), and $Q$ is the salt flow rate ($m^3/s$).

## 4. Flow System Design

In previously reported work [9], we established a reactor design that enhances the surface area of electrodes to volume of reactor for this application, which was an annular plug flow reactor. The finalized design for a laboratory-scale reactor based on this concept is shown in Figure 2 (left) along with a finite element model to predict thermal stresses (Figure 2, right).

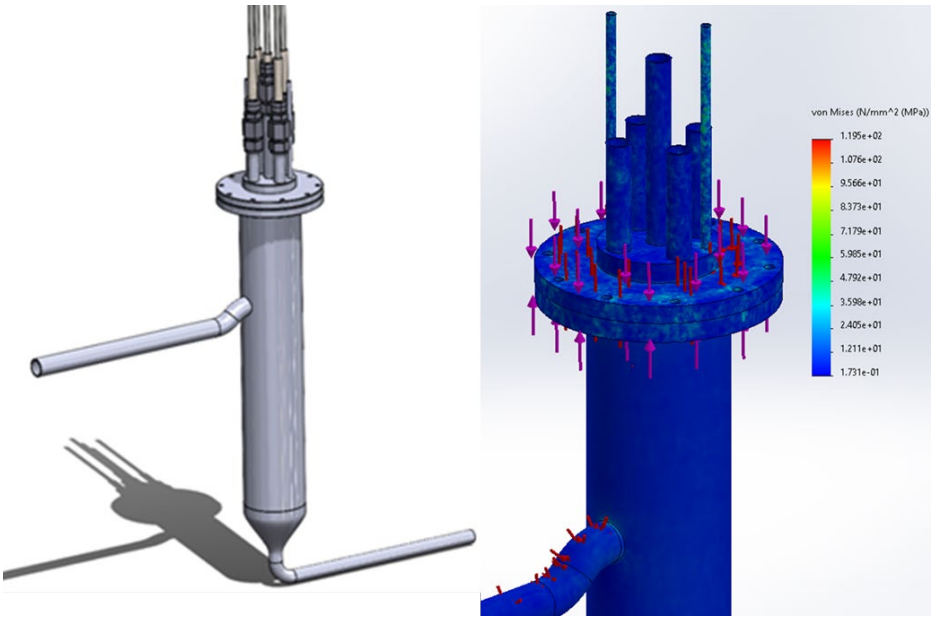


**Figure 2**. SolidWorks drawing of purification vessel (left) and thermal stress analysis of purification vessel (right).

From Figure 2, the reactor consists of a body built from an 18-in. long, 3-in. schedule 40 pipe and a custom ConFlat (CF) flanged lid; the entire vessel is made out of Hastelloy C-276. The reactor is bottom fed with a weir 6 in. from the lid to ensure steady discharge and electrode immersion in the salt. The area ratio of outlet to inlet was designed to be 1.84. The custom CF flange at the top houses ensures a leak-tight seal while allowing several ports to vary number of electrodes and configuration. The ports house the electrodes, a thermocouple,

and a pressure relief valve to ensure no dangerous amounts of hydrogen will build up in the headspace. Three heat shields are attached to the bottom of the lid with the studs staggered to minimize conduction (based on previous work [10]). Furthermore, the highest stress predicted was 119.5 MPa, which is well below the allowable stress of 154 MPa for Hastelloy C276 at 500 °C.

The electrodes to be used consist of the W or Mg rod in an alumina sheath and castable ceramic based on the work by Vidal et al. [11]. The alumina sheath ensures electrical insulation from the electrodes and the reactor body.

To test the purification reactor, we designed a flow system to pump salt through the purification cell in a laboratory setting. The flow system uses two Hastelloy C276 vessels for salt storage and a C276 transfer line with the purification cell located within the transfer line. The complete flow system design is shown in Figure 3 (left), along with a finite element model of the transfer lines (Figure 3, right).

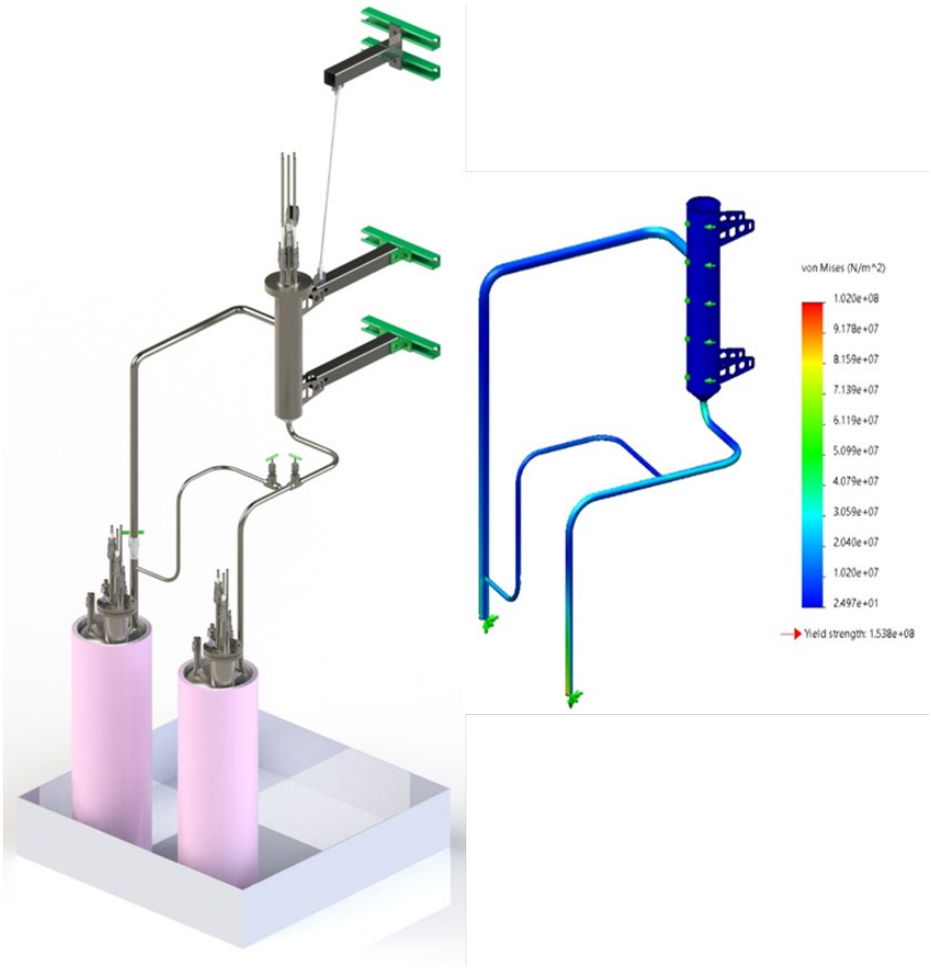


**Figure 3**. SolidWorks drawing of full flow system (left) and thermal stress analysis of transfer lines (right).

From Figure 3, the highest stress predicted (102 MPa) is below the maximum allowable stress of Hastelloy C276 at 500 °C. During experiments, one C276 storage vessel will be emptied, and the other vessel will be filled with molten salt (20–30 kg) with introduced $MgOH^+$ impurities. Pressure will be applied to the overhead space of the full vessel and a vacuum will be pulled on the empty vessel to cause flow of salt through the transfer line and

purification cell. The rate of mass change allows quantification of molten salt flow rate. Each vessel includes a custom CF flange to house electrodes for electrochemical quantification of impurity concentration throughout the experiment.

The vessels and transfer line will be trace heated and insulated to achieve the desired testing temperature of 500 °C. Vessel heaters will be laser-cut serpentine alternative-current heaters with estimated 433-in. conduction length, 0.4-in. width, 0.0187-in. thickness, alloy 800H, and estimated 2.5 Ohm resistance. The insulation layers will include two layers of mica sheet to electrically insulate the heaters from the vessels while Kaowool and Pyrogel will thermally insulate the vessels. The transfer lines will be heated using a combination of AC heating tape and direct-current trace heating. The transfer lines will be insulated with Kaowool and Pyrogel (not shown in the figure).

## 5. Estimated Flow System Performance

The Sherwood number and mean residence times were calculated for the purification cell in the flow system and shown in Figure 4.

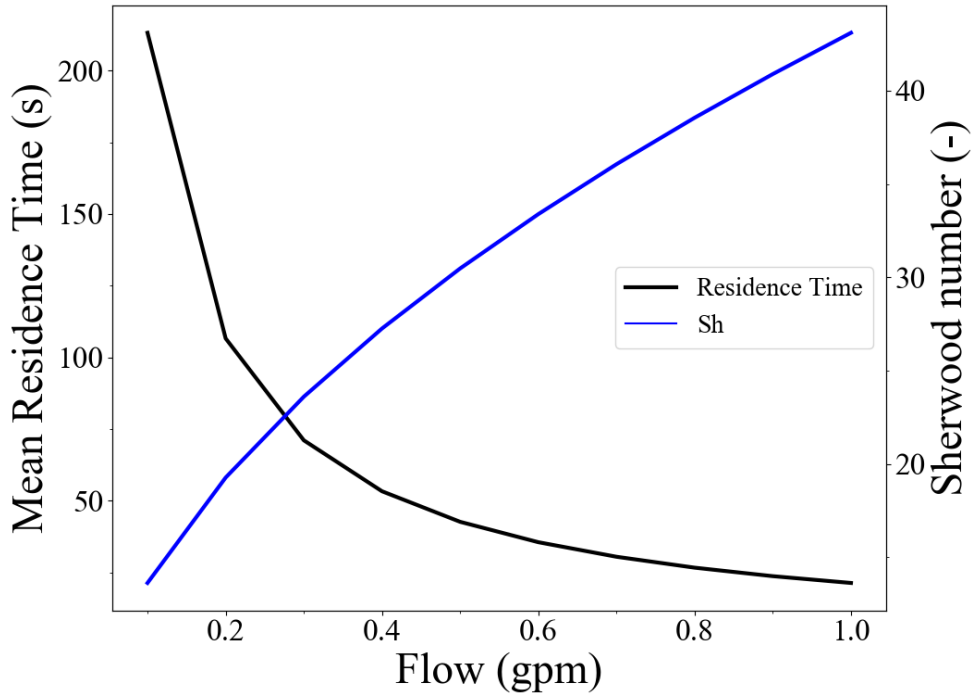


**Figure 4**. Predicted Sherwood number and mean residence number vs. flow rate.

From Figure 4, increasing the flow rate from 0.1 to 1 gpm results in the Sherwood number increasing from 14 to 43. Therefore, the estimated current density ranges from 1.1 to 3.4 A/cm$^2$. While increasing the flow rate enhances the mass transfer of $MgOH^+$, the mean residence time inside the reactor decreases significantly. It is therefore expected that the optimum purification rate will be at lower flow rates.

## 6. Conclusion

We have designed an electrochemical flow cell for evaluation of purification of molten salts in a laboratory setting under flowing conditions. Furthermore, we have designed a simple system for pumping salt through this cell. This work is a step towards designing an online corrosion solution for molten chloride salt systems in industrial settings.

## Data availability statement

The data that support the findings of this study are available from the corresponding author upon reasonable request.

## Author contributions

Liam Witteman: Writing – Original Draft; Writing – Review and Editing; Methodology; Visualization; Formal Analysis. Kerry Rippy: Review and Editing; Funding Acquisition; Project Administration; Conceptualization. Evan Ogren: Visualization; Writing – Original Draft; Software. Mark Anderson: Project Administration; Supervision. Patrick Taylor: Supervision; Writing – Review and Editing. Judith Vidal: Supervision; Writing – Review and Editing.

## Competing interests

The authors declare no competing interests.

## Funding

This work was authored in part by the National Renewable Energy Laboratory, operated by Alliance for Sustainable Energy, LLC, for the U.S. Department of Energy (DOE) under Contract No. DE-AC36-08GO28308. Funding provided by U.S. Department of Energy Office of Energy Efficiency and Renewable Energy Solar Energy Technologies Office grant CSP #35931 as well as the Colorado School of Mines/NREL Advanced Energy Systems Graduate Program. The views expressed in the article do not necessarily represent the views of the DOE or the U.S. Government. The U.S. Government retains and the publisher, by accepting the article for publication, acknowledges that the U.S. Government retains a nonexclusive, paid-up, irrevocable, worldwide license to publish or reproduce the published form of this work, or allow others to do so, for U.S. Government purposes.

## Acknowledgement

We would like to thank Matthew Earlam and Stephen James for their thoughtful discussions during the initial design state of the project.

## References

1. A.M. Gray, “Corrosion Mitigation of Nickel Alloy Metals in Molten Chloride Salts.” Doctoral dissertation. Tucson, AZ, USA: The University of Arizona 2021, https://repository.arizona.edu/handle/10150/661627.
2. A.M. Kruizenga, “Corrosion Mechanisms in Chloride and Carbonate Salts.” Albuquerque, NM, USA: Sandia National Laboratories 2012, https://energy.sandia.gov/wp-content/gallery/uploads/SAND2012-7594-Corrosion-Mechanisms-in-Chloride-and-Carbonate-Salts-Kruizenga.pdf.
3. Y. Zhao, N. Klammer, and J. Vidal, “Purification Strategy and Effect of Impurities on Corrosivity of Dehydrated Carnallite for Thermal Solar Applications,” RSC Adv., 9(71), pp. 41664–41671, Dec. 2019, https://doi.org/10.1039/C9RA09352D.
4. Y. Zhao, and J. Vidal, “Potential Scalability of a Cost-Effective Purification Method for MgCl2-Containing Salts for next-Generation Concentrating Solar Power Technologies,” Sol. Energy Mater. Sol. Cells, 215, p. 110663, June 2020, https://doi.org/10.1016/j.solmat.2020.110663.
5. W. Ding, J. Gomez-vidal, A. Bonk, and T. Bauer, “Molten Chloride Salts for next Generation CSP Plants: Electrolytical Salt Purification for Reducing Corrosive Impurity Level,”

Sol. Energy Mater. Sol. Cells, 199, pp. 8–15, Sept. 2019, https://doi.org/10.1016/j.solmat.2019.04.021.
6. W. Ding, A. Bonk, J. Gussone, and T. Bauer, “Cyclic Voltammetry for Monitoring Corrosive Impurities in Molten Chlorides for Thermal Energy Storage,” Energy Procedia, 135, pp. 82–91, Oct. 2017, https://doi.org/10.1016/j.egypro.2017.09.489.
7. J. Guo, N. Hoyt, and M. Williamson, “Multielectrode Array Sensors to Enable Long-Duration Corrosion Monitoring and Control of Concentrating Solar Power Systems,” J. Electroanal. Chem., 884, p. 115064, March 2021, https://doi.org/10.1016/j.jelechem.2021.115064.
8. C.S. Un, E.B. Denton, H.S. Gaskill, and G.L. Putnam, “Diffusion-Controlled Electrode Reactions,” Ind. Eng. Chem., 43(9), pp. 2136–2143, Sept. 1951, https://doi.org/10.1021/ie50501a045.
9. K. Rippy, L. Witteman, A. Monasterial, P. Taylor, and J. Vidal, “Geometric Optimization of an Electrochemical Purification Cell to Prevent Corrosion in CSP Plants During Operation,” *SolarPACES Proceedings* 2022
10. F. Liu, “Fundamental Electrochemical Study on Neodymium Molten,” Golden, CO, USA: Colorado School of Mines, 2019, https://hdl.handle.net/11124/173998.
11. J.C. Gomez-Vidal and E. Morton,“Castable Cements to Prevent Corrosion of Metals in Molten Salts,” Sol. Energy Mater. Sol. Cells, 153, pp. 44–51, Aug. 2016, https://doi.org/10.1016/j.solmat.2016.04.009.